How to cite: *Angew. Chem. Int. Ed.* **2025**, *64*, e202418291
doi.org/10.1002/anie.202418291

Small Molecule Modulators

Crafting Molecular Tools for 15-Lipoxygenase-1 in a Single Step

*Anastasia Louka[+], Ntaniela Spacho[+], Dimitris Korovesis, Konstantinos Adamis, Christos Papadopoulos, Eirini-Eleni Kalaitzaki, Nektarios Tavernarakis, Constantinos G. Neochoritis, and Nikolaos Eleftheriadis**

Abstract: Small molecule modulators are powerful tools for selectively probing and manipulating proteins in native biological systems. However, the development of versatile modulators that exhibit desired properties is hindered by the lack of a rapid and robust synthetic strategy. Here, we develop a facile and reliable one-step methodology for the generation of multifunctional toolboxes encompassing a wide variety of chemical modulators with different desired features. These modulators bind irreversibly to the protein target *via* a selective warhead. Key elements are introduced onto the warhead in a single step using multi-component reactions. To illustrate the power of this new technology, we synthesized a library of diverse modulators designed to explore a highly challenging and poorly understood protein, human 15-lipoxygenase-1. Modulators made include; activity-based/photoaffinity probes, chemosensors, photocross-linkers, as well as light-controlled and high-affinity inhibitors. The efficacy of our compounds was successfully established through the provision of on demand inhibition and labeling of our target protein *in vitro*, *in cellulo* and *in vivo;* thus, proving that this technology has promising potential for applications in many complex biological systems.

Introduction

Small molecule modulators play a crucial role in chemical biology, where they are used to probe and manipulate biological processes at the molecular level.[1–3] These molecules typically have low molecular weight and are equipped with certain functionalities that render them ideal for studying specific molecular targets within complex biological systems.[4] Commonly reported types of these "smart" bioactive molecules include covalent inhibitors,[5] activity-/affinity-based probes,[6,7] sensors,[8] photobiological switches[9] and photoactivated cross-linkers.[10] Although these modulators provide numerous advantages in understanding biological processes and developing therapeutic interventions, they also have some disadvantages, such as; lack of specificity, poor pharmacokinetics, and, most importantly, challenges incurred during development.[11,12] Often, the discovery and development of small molecule modulators can be time-consuming and costly, requiring extensive screening and optimization. In addition, poor development may also yield compounds that exhibit off-target effects, low bioavailability and limited cell membrane penetration, leading to questionable results.[4] A generic and reliable methodology which could be consistently applied to the development of new tools capable of selectively targeting proteins within complex biological systems, would be game-changing.

In our prior research, we encountered many of the aforementioned challenges while developing the first activity-based probes for the enzyme human 15-lipoxygenase-1 (15-LOX-1).[13] 15-LOX-1 belongs to lipoxygenase family and catalyzes the insertion of oxygen into polyunsaturated fatty acids, such as, arachidonic (AA) or linoleic acid (LA), resulting in signaling inflammatory molecules.[14] This enzyme possesses a regulatory role in respiratory and other inflammatory diseases, such as asthma and inflammatory bowel disease (IBD),[14–17] various CNS diseases like ischemic strokes, Alzheimer's and Parkinson's,[16,18–20] as well as in many aspects of various cancers, including; leukemia and colon cancer.[21–30] It has been proposed that 15-LOX-1 is involved in two different mechanistic pathways; it both causes inflammation and can trigger apoptosis (ferroptosis).[31–40] Full understanding and exploitation of the role of 15-LOX-1 in these highly complex pathways will not be possible without "smart" molecules that modulate its function. For this reason, we selected this challenging and complex enzyme as the model protein to test the scope of

[*] Dr. A. Louka,[+] N. Spacho,[+] K. Adamis, C. Papadopoulos, E.-E. Kalaitzaki, Prof. C. G. Neochoritis, Prof. N. Eleftheriadis
Department of Chemistry
University of Crete
Voutes, 70013 Heraklion, Greece
E-mail: n.eleftheriadis@uoc.gr

Dr. D. Korovesis, Prof. N. Tavernarakis
Institute of Molecular Biology and Biotechnology
Foundation for Research and Technology-Hellas
Nikolaou Plastira 100, 70013, Heraklion, Greece

Prof. N. Tavernarakis
Division of Basic Sciences, School of Medicine
University of Crete
Voutes, 70013 Heraklion, Greece

[+] These authors contributed equally to this work.

our new rational methodology and its ability to afford a variety of tools necessary for probing structure and function, in just one synthetic step. Success in this difficult case would indicate potential for future applications of our technology in other biological protein targets.

We have recently revealed that bis-alkyne (BA) substrate mimics bind covalently to 15-LOX-1 through a possible mechanism *via* a radical allenic intermediate.[13,41,42] Leveraging this observation, we sought to harness this unit as a warhead to covalently anchor different modulators to the enzyme's active site (Figure 1). We envisaged generating diverse libraries of BA modulators (BAMs) by employing a suitably adapted BA unit as a partner in a number of powerful and highly economic (atom/time/energy) multicomponent reactions (MCRs). MCRs are uniquely suited to rapid expansions into new chemical space because, in just one step, a large variety of scaffolds/motifs can be accessed and these products can have a range of highly variable properties and desired features. Herein, we have employed a BA covalent anchor bearing a suitably spaced reactive functional group (an aldehyde) in 2CRs or MCRs, with the other components being fluorescence compounds, benzophenone, azobenzene and (acyl)hydrazone derivatives, allowing us to isolate after a single synthetic operation the corresponding activity-based probes, chemosensors, photocrosslinkers, as well as light-controlled and high affinity inhibitors (Figure 1).

Results and Discussion

Strategic Design of Effective Modulators

We developed a versatile synthetic strategy designed to explore an extensive chemical space through the efficient generation of diverse small molecule modulators. The core of this generic strategy involves a modular approach that utilizes a covalent anchor (herein the BA moiety) with the reactive group (herein the aldehyde). This setup allows for the incorporation of various bioactive moieties *via* 2CRs and MCRs. Our approach leverages the flexibility of MCR chemistry, including Groebke-Blackburn-Bienaymé (GBB-3CR), Passerini (P-3CR), Ugi (U-4CR), and Ugi tetrazole (UT-4CR) reactions, to introduce a wide range of functional groups and structural motifs. This strategy facilitates the rapid synthesis of complex scaffolds with diverse physicochemical properties, enabling the potential generation of a vast array of compounds with varying shapes, molecular weights, and lipophilicities, laying the groundwork for identifying effective binders (herein 15-LOX-1 inhibitors).

The portfolio of tools we were targeting had been rationally designed guided by a virtual database of known 15-LOX-1 inhibitors (>6.100) we had constructed in-house (Supporting Information, Dataset 1). This database enables exploration of the key structural elements and potential of each compound based on physicochemical properties and molecular features. Our analysis revealed that the enzyme has the tendency to bind tightly (IC_{50} < 5 μM) to lipophilic, linear molecules with large molecular weight and polar surface area (clogP > 5, shape index > 0.5, MW > 500 Da, tPSA > 100) (Figure 2a). Moreover, in order to utilize the most active MCR components when synthesizing our modulators, we investigated separately the inhibitory activity of amine, carboxylic acid and isocyanide fragments against 15-LOX-1 (Figure 2b). From the database, we identified the most potent amine and carboxylic acid fragments (MW < 200 Da), revealing diverse pharmacophore models, which we then employed in our syntheses (Figure 2b). Since isocyanides have not previously been reported as 15-LOX-1 inhibitors, and, therefore, were not covered by our database, we have performed an inhibitory screening of a small library against our enzyme, identifying few relatively active isocyanide fragments (IC_{50} < 50 μM) (Figure 2b).

Expanding the Chemical Space

We began with the facile synthesis from 5-hexyn-1-ol of the common starting point for all our portfolio of tools; namely, diynal building block **BAM1**. 5-Hexyn-1-ol was oxidized

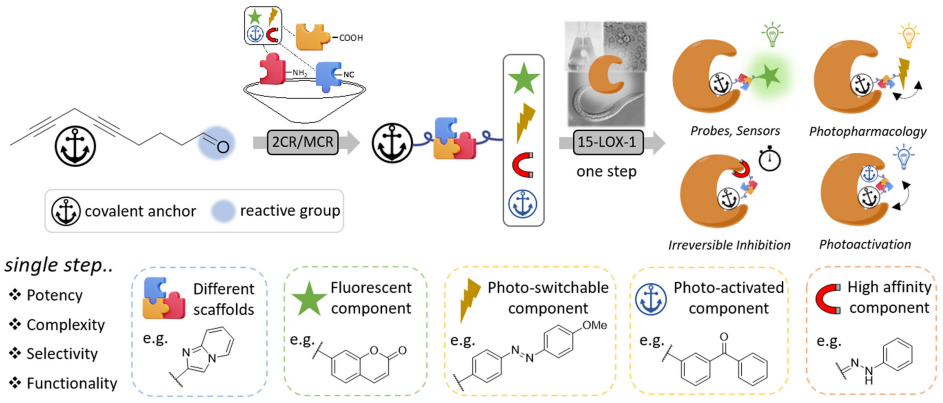

Figure 1. Strategy for the development of BAM compounds. The covalent anchor (BA) was incorporated through a reactive group (aldehyde) in 2CRs and MCRs to yield BAM probes, sensors, photocrosslinkers, as well as light-controlled and high-affinity inhibitors. Modulation of 15-LOX-1 activity occurred following a time-dependent binding of the respective BAM compound, accomplished in a single step.

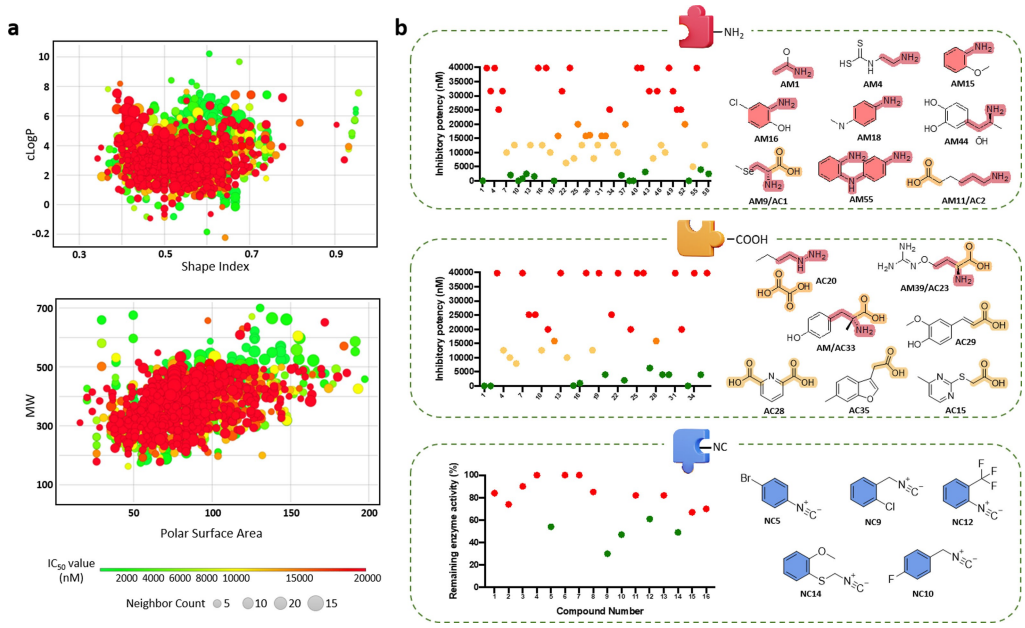

Figure 2. Rational development of potent binders. a) 2D plot analysis of previously identified 15-LOX-1 inhibitors, based on lipophilicity (clogP) and shape index, as well as the molecular weight (MW) and the polar surface area. The size and the color of every dot represents the quantity of similar scaffolds and the inhibitory value (nM), respectively. b) Representation of the inhibitory potency of amine (nM), acid (nM) and isocyanide (at 50 μM) fragments against 15-LOX-1. The active fragments are presented and the common structural component is highlighted. The color gradient represents the inhibitory potency, ranging from high (green) to low (red).

using PCC to yield 5-hexynal (**C1**). Subsequently, the desired compound **BAM1** was efficiently synthesized through a C–C Sonogashira-type coupling reaction with 1-bromo-2-butyne. Compound **BAM1** has an aldehyde functional group on one terminus of the molecular chain that can readily be engaged in condensation reactions with primary amines, yielding in a straightforward manner imines (Figure 3a). To employ the correct linear shape and after optimizing the reaction conditions, we achieved efficient imine formation between **BAM1** and three disparate amines, yielding imines **BAM2-4**. In order to generate more complex scaffolds with the suitable physicochemical properties and introduce new modalities *via* multiple key components, each time in a single step, we employed MCR chemistry. To this end, we elegantly converted fluorescein, coumarin and benzophenone moieties into isocyanide components (Supporting Information). Utilizing a GBB-3CR reaction, straightforward access to imidazo[1,2-*a*]pyridines was provided in only one step.[43] In this 3-component reaction, we used **BAM1**, 2-aminopyridine, and four different isocyanides, to furnish compounds **BAM5-8**. Next, the P-3CR was harnessed as an alternative 3-component reaction. It involves a carbonyl compound, a carboxylic acid and an isocyanide and yields products characterized by a more compact and less intricate core. In all cases, **BAM1** reacted with acetic acid and different isocyanides to yield compounds **BAM9-11,13,14**. In case of **BAM12**, to introduce the azobenzene moiety, acetic acid was replaced by azobenzoic acid **5**. Finally, to further investigate the scope and limitations of the new BAM compounds, we attempted to synthesize compounds with increased complexity. The U-4CR reaction was performed between **BAM1**, acetic acid and different isocyanides and amines, resulting in the formation of the compounds **BAM15-17**. We also employed the UT-4CR.[44] The tetrazole ring imparts valuable properties to drug molecules, influencing their bioavailability, metabolic stability and target interactions.[44,45] **BAM18** and **19** were synthesized, using **BAM1**, $TMSN_3$, isocyanocyclohexane and benzylamine or 2-isocyano-2-methylpropane and propan-1-amine, respectively. All the synthesized BAM compounds were isolated in good to excellent yields (Figure 3b). Additionally, control compounds (**C1–11**, Figure 4e) lacking the bis-alkyne moiety or other important structural elements, were also purchased or synthesized (Supporting Information).[46]

Inhibitory Characterization of BAMs

We next sought to characterize their binding potencies and kinetics. The newly synthesized BAM compounds were screened for inhibition against human 15-LOX-1 as described previously.[13,47–50] IC_{50} values were determined for all the compounds, which showed potencies in the low-micromolar range (Figure 3b, 4d). In line with our initial cheminformatic analysis, we have found that linear lipophilic compounds proved to be more potent, with **BAM3**, for example, having an IC_{50} of 0.15 μM. Furthermore, the identified pharmacophore components from the fragments (e.g. 4-bromophenyl isocyanide, propylhydrazine, acetic acid) seem to contribute positively in the inhibitory activity of compounds, such as, **BAM5** and **BAM11**. Conversely,

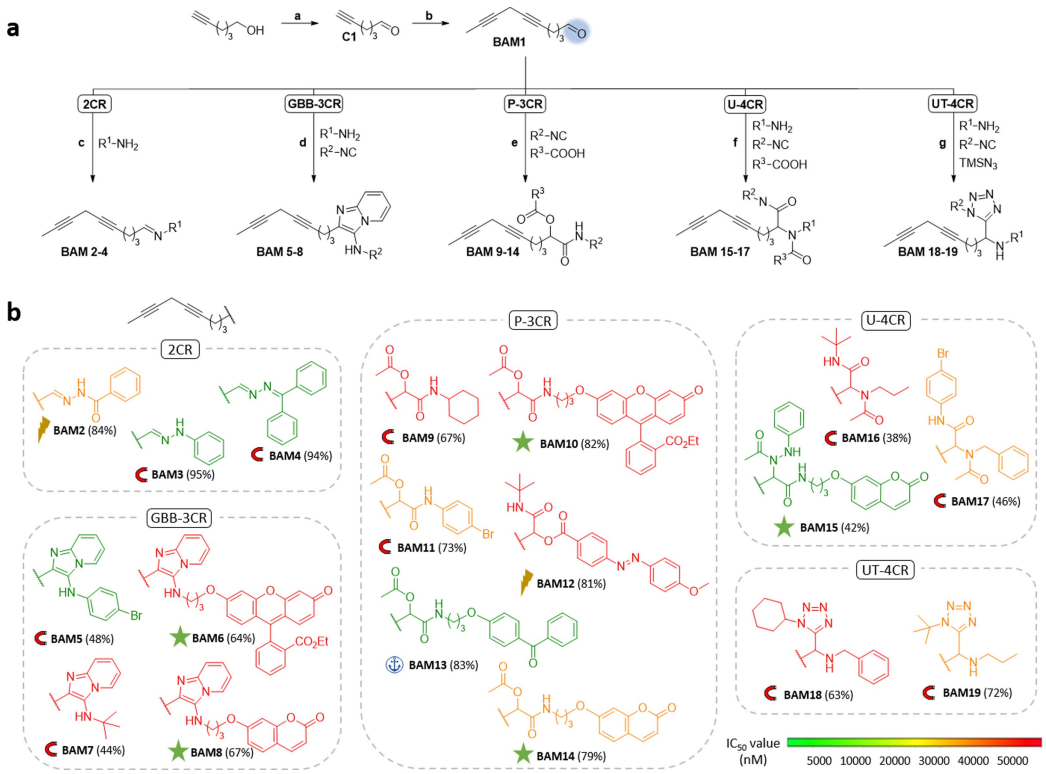

Figure 3. Synthesis of BAM compounds. a) Reagents and conditions: a) PCC, dry DCM, rt, 2 h; b) 1-bromo-2-butyne, CuI, NaI, K_2CO_3, DMF, rt, 48 h; c) hydrazine, MeOH, rt or benzohydrazide, THF, rt, 16 h; d) 2-aminopyridine, isocyanide, $Sc(OTf)_3$, MeOH, r.t. or 45 °C, 16–24 h; e) carboxylic acid, isocyanide, DCM, rt, 12 h; f) amine, isocyanide, carboxylic acid, MeOH, r.t., 16–24 h; g) amine, isocyanide, $TMSN_3$, MeOH, 45 °C, 16–24 h. b) The libraries of the synthesized BAM compounds obtained from different reactions with their corresponding yields. The color represents the inhibitory value (IC_{50} in nM scale, 20 min preincubation) as shown. The symbol represents the potential application of the compound, lightning bolt: photo-switchable; magnet: inhibitor; star: probe; anchor: cross-linker.

branched and bulky components (e.g. tert-butyl- or cyclohexyl isocyanide) demonstrated lower activity, as seen in **BAM9** and **BAM18**.

As expected from our conceptual design, the IC_{50} values for all BAM compounds proved to be time-dependent, with a difference observed between preincubation times of 10 and 20 min, indicating irreversible inhibition (Figure 4b, d). This difference varies between the BAM compounds, from slightly, in the case of **BAM3**, to a lot, in the case of **BAM2** (Figure 4b, d), possibly as a result of their initial binding pose. The same is not true for the control compounds missing either the BA unit or where the BA has a substituted methylene group (Figure 4b, e and Figure S1). Further analysis using Lineweaver–Burk plots showed non-competitive inhibition for **BAM1** (Figure 4a and Figure S2). This result supports the model in which the compounds bind irreversibly through the BA moiety. To verify this and further investigate the mechanism of covalent modification, we pre-incubated **BAM3** with purified 15-LOX-1, followed by an in-gel digestion protocol and mass spectrometry (MS)-based proteomics,[51] mapping for the first time the preferred target residues from binding site of human 15-LOX-1. The analysis identified the tryptic peptide sequence [YTLEINV-RAR] with amino acids 395–404 displaying a mass increase of +230 Da, corresponding to an adduct of **BAM3**. Our findings pointed out the area at the entrance of the active site, close to the iron and specifically at the amino acids **Y395**, **T396** and **L397**, as the attachment site (Figure 4c and Figure S4, 5). These findings align with our current structural understanding of 15-LOX-1, suggesting that the formation of the radical allenic intermediate, which requires iron, preferentially occurs near these residues due to their proximity to the active site.

Another remarkable finding is that the complexity achieved with some BAM compounds translates into substrate-specific inhibition, which may impact the regulation of specific mediators without impacting the biosynthesis of others formed from different fatty acids.[52] While the more compact **BAM5** exhibits higher potency when LA was used as substrate (1.5 folds), the extended **BAM10** behaves conversely, demonstrating inhibitory potency only for the oxygenase activity of AA (14 fold) (Figure 4f). Finally, we examined the target selectivity profile of our most potent inhibitor **BAM3**, between human 15-LOX-1 and soybean LOX, which is an isoenzyme from plants with high structural similarity.[53] We found a 4-fold difference in the inhibitory potency in favor of human 15-LOX-1, showing that **BAM3** has a significant degree of selectivity (Figure 4g).

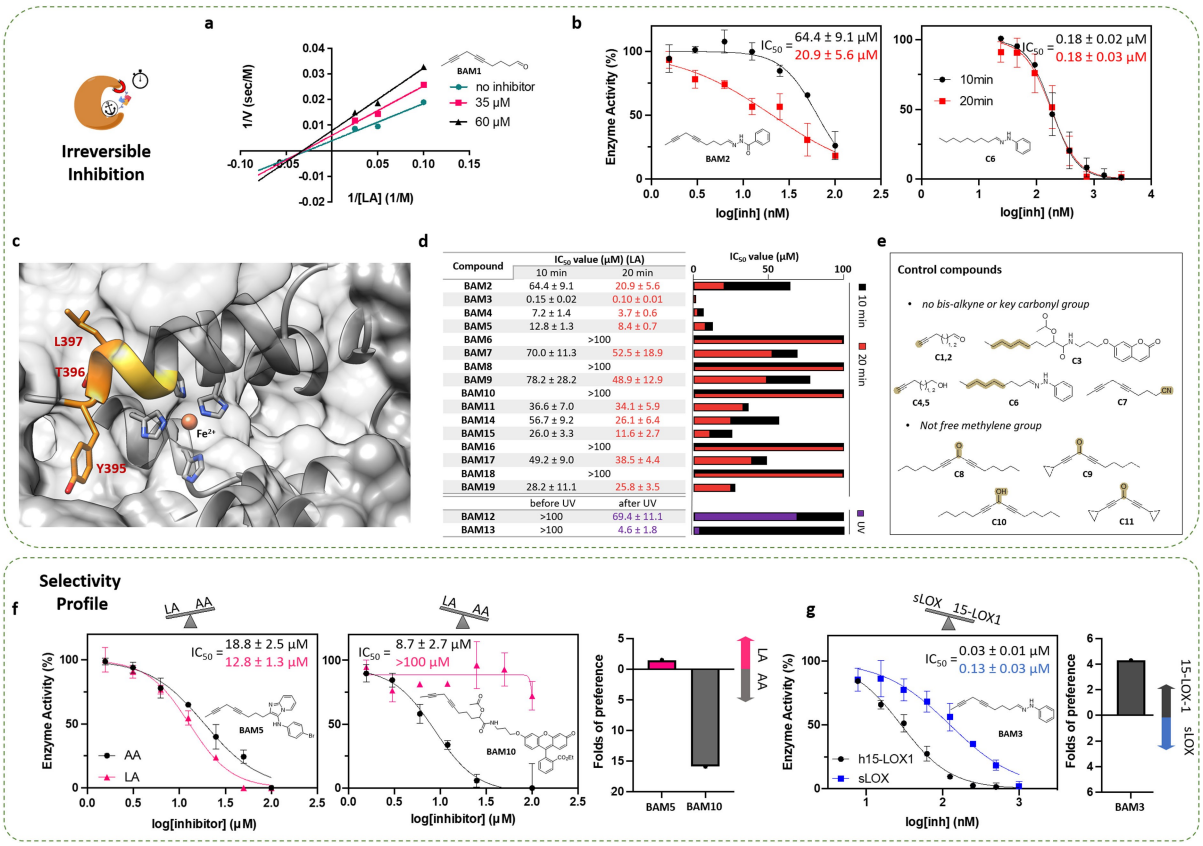

Figure 4. Exploring the nature of inhibition. a) Lineweaver–Burk plot of BAM1. b) Inhibition of 15-LOX-1 with the IC_{50} graphs of 10 and 20 minutes of incubation with BAM2 (left) and C6 (right). c) The active site of human 15-LOX-1. Residues Y395, T396 and L397, identified by MS experiments, are shown in orange sticks. d) Table of IC_{50} values (10 and 20 minutes) of the synthesized BAM compounds. All values are reported with their standard deviation. e) Chemical structures of control non-covalent compounds, with key structural elements highlighted. f) IC_{50} curves showing the different inhibitory potencies of BAM5 (left) and BAM10 (right), using AA or LA as substrates in the enzymatic reaction. g) Inhibition of 15-LOX-1 and soybean LOX with the IC_{50} curves after 30 min incubation with the compound BAM3. All experiments were performed in triplicates ($n = 3$), and the standard error is reported.

Exploring the Features and Potential of BAMs

Our versatile portfolio of BAM tools covers a wide range of applications in chemical biology, where they can be used to probe and manipulate biological systems at the molecular level. With this new generation of activity-based probes, we are able to detect our enzyme in a single step, without the need of additional biorthogonal reactions for protein labeling.[13,47–49,54] Using our rapid and innovative synthesis, we have developed a range of BAM probes, having different molecular features and fluorescence tags (Figure 3b). An appropriate probe must exhibit good and fast binding to the target-enzyme, alongside optimum physicochemical properties.[55] **BAM10** and **BAM14** proved to be our best examples, carrying a fluorescein and coumarin tag, respectively, with the necessary linker. After characterizing their time dependent inhibitory potency and absorption/emission spectra (Figure 5a, b), **BAM10** or **BAM14** were applied in labeling experiments on the recombinant purified enzyme 15-LOX-1. Initially, the probe was incubated for a short time with the purified enzyme, followed by an acetone precipitation. **BAM14** clearly labeled the enzyme 15-LOX-1 in contrast to the control experiment, while the excess probe remains in the supernatant (Figure 5c). Moreover, reduced labeling of the enzyme (dot-blot experiments) was observed when **ThioLox**, a known 15-LOX-1 inhibitor,[48] was applied prior to the probe **BAM10**, whereas a control experiment without 15-LOX-1 demonstrated no differences (Figure 5c and Figure S6). This result demonstrates an activity-based labeling of 15-LOX-1 in a single-step, using this approach. Another remarkable feature of **BAM14** is its ability to sense Fe^{3+}, highlighting its potential as an advanced molecular chemosensor for ferroptosis.[56,57] In the presence of an accumulated amount of iron, the absorbance of **BAM14** increased (Figure S7) while at the same time its fluorescence decreased accordingly due to specific quenching (Figure 5d).

Subsequently, employing the principles of high-precision photo-pharmacology,[8,58] our novel light-controlled compounds gave us access to on demand local photoactivation of 15-LOX-1 inhibition. We incorporated azobenzene and (acyl)hydrazones moieties into our BAM compounds (Figure 3b), aiming for easy geometric conversion upon UV irradiation which should allow us to harness the significant differences in inhibitory potency that are predicted to exist

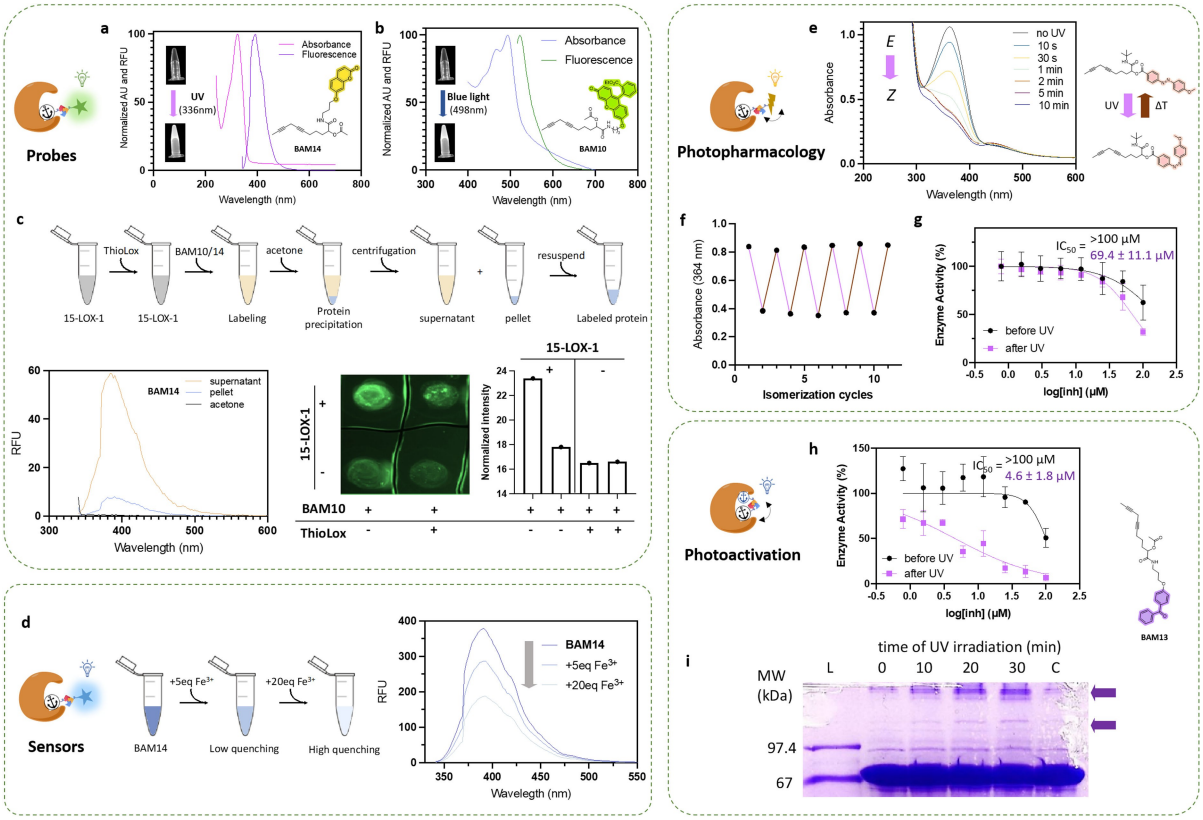

Figure 5. The photo-induced features of BAMs. a) The absorption/emission spectra of BAM14. b) The absorption/emission spectra of BAM10. c) The fluorescence of BAM14 (left) or BAM10 (right) after labeling of 15-LOX-1. Emission spectra for the supernatant (yellow) and resuspended pellet (cyan) after acetone precipitation. A blank sample of acetone is represented with black (left). Dot-blot (fluorescence) of BAM10-treated 15-LOX-1, with or without preincubation with ThioLox. Control experiments in the absence of 15-LOX-1 is shown in the bottom. Experiments were performed in duplicates ($n=2$). d) Emission spectra of BAM14 in presence of 5 and 20 equivalents of Fe^{3+}. e) Absorption spectra of BAM12 showing the conversion from the *E* to *Z* conformation upon increasing exposure time of UV light, and return to the E conformation after heat treatment. f) Reversible photochromism of BAM12 (5 cyclic irradiations). g) Inhibitory potency of BAM12 before and after UV irradiation. h) Inhibitory potency of BAM13 before and after UV irradiation. All IC_{50} experiments were performed in triplicates ($n=3$), and the standard error is reported. i) SDS-page reveals increasing crosslinked protein species, after incubation of BAM13 (or DMSO: C) with cell lysate (with overexpressed 15-LOX-1) and application of UV irradiation for 0, 10, 20 and 30 min (L: protein ladder).

between the *E*- and *Z*-conformer. **BAM12** emerged as the optimal choice, displaying swift isomerization from the *E*- to *Z*-conformer within only 2 min (!) under UV irradiation at 365 nm with reversion to the *E* conformer upon heating treatment (10 min at 40 °C) (Figure 5e, f and Figure S8). To investigate the above, we used NMR characterization to look at the products obtained after UV irradiation, revealing a 1:1 ratio of *E*- to *Z*-isomers with the appearance of distinct characteristic peaks (Figure S9). This light-induced isomerization leads to structural changes that consequently modify the inhibitory activity. Indeed, the inhibitory potency of **BAM12** increases significantly when it acquires the *Z*-conformation (Figure 5g). The advantage and uniqueness of our BAM-light-controlled inhibitor lie in the covalent nature of the anchoring that enables prolonged therapeutic efficacy at reduced doses.[59]

In addition, we developed a BAM photo-crosslinker, functionalizing a benzophenone moiety *via* our novel methodology (Figure 3b). The **BAM13** compound is switched from bio-silent (IC_{50} >100 µM) to bioactive upon UV irradiation (10 min), with an IC_{50} value of 4.8 ± 1.8 µM (Figure 5h). Control experiments that verify equal enzyme activity upon UV irradiation have been successfully performed (Figure S10a). To explore the potential of **BAM13** to be used as a protein crosslinker, we performed gel-based experiments using 15-LOX-1-overexpressing cell lysates treated with **BAM13** and subjected to UV irradiation for different exposure times. We observed three distinct protein bands that increased in intensity in an irradiation time-dependent manner, which were not visible in the negative control (Figure 5i and Figure S10b). The bands with MW higher than that of 15-LOX-1 (indicated with arrows in Figure 5i) suggest that the benzophenone of **BAM13** may crosslink to protein partners of 15-LOX-1, including potential homo-oligomers or interaction partners. These findings indicate that **BAM13** may be a valuable tool for investigating 15-LOX-1 oligomerization and mapping its interactome in complex biological systems.

Applications of BAM Compounds in a Cellular Model

We next explored the applicability of our newly synthesised **BAM10** in a cellular model. Previously, 15-LOX-1 has been visualized in cells using a biotinylated probe, necessitating additional steps such as cell fixation and subsequent fluorescent labelling *via* conjugation to streptavidin.[41] The presence of the fluorescein moiety on **BAM10** on the other hand eliminates this need and may enable live-cell imaging. RAW 264.7 macrophage cells that express endogenous 15-LOX-1 were chosen as a model system, as in previous studies.[41,47,48,60] Initially, we evaluated the cell permeability of **BAM10** by treating live cells (*in situ*, on the microscope) and immediately recording images to follow its cellular uptake. **BAM10** was taken up by cells rapidly and reached saturation within 8 minutes (Figure S11). On the other hand, free fluorescein was impermeable within the timeframe of our experiment (Figure S12), suggesting that our BA scaffold is highly permeable. Thus, **BAM10** is a cell-permeable probe suitable for live cell imaging.

In cellulo target engagement of 15-LOX-1 by **BAM10** was then investigated in a cell-based competition assay (Figure 5a, top) using a confocal microscope. We reasoned that if the observed labelling by **BAM10** corresponds to 15-LOX-1 *in cellulo* engagement, then competition with 15-LOX-1 inhibitors will result in lower total cell intensity; especially, if this occurs in dose-dependent manner. As competitors we used **BAM3**, as an untagged derivative of **BAM10**, and ThioLox.[48] 5 μM of **BAM10** was used in the competition assay, as this is close to its IC_{50}. While competition with an equimolar concentration of either **BAM3** or **ThioLox** was not significant, increasing the concentration of either competitor 10-fold, resulted in a reduction of **BAM10** fluorescence intensity (Figure 6b, c and Figure S13). For the latter competitor, the intensity decreased almost to background levels, indicating that **ThioLox** has superior permeability and/or stability in cells compared to **BAM3** (given that both have high binding potency, low IC_{50}). These results indicate that **BAM10** engages with 15-LOX-1 in live cells.

Our MS and acetone precipitation experiments showed that **BAM10** binds covalently with purified 15-LOX-1. In order to evaluate whether this reaction takes place in the complex environment of cells, we took images of live cells following excessive washes of **BAM10** (following a 16-minute incubation). While the total **BAM10** fluorescence had decreased following the washes, our analysis clearly indicated that **BAM10** labelling is retained for at least 30 minutes post washing (Figure S14). To further explore whether this is due to binding, we designed an irreversibility assay where live cells are initially incubated with **BAM10** for various durations and then treated with **ThioLox** for 1 hour before imaging (Figure 6a, bottom). In line with our permeability assay, **BAM10** intensity without competition reached saturation at just 3.75 minutes (it is important to note that **BAM10** incubation was at 37 °C in this instance, as opposed to the permeability assay which was performed at rt) and remained constant even in the 2-hour time period. On the other hand, **BAM10** fluorescence intensity in samples with a 10-fold excess of ThioLox was highly dependent on time. The higher the pre-incubation time of **BAM10**, the less effective the competition from **ThioLox** became. Given that **BAM10** labelling does not increase with time, collectively these results indicate that prolonged pre-incubation may enable a higher percentage of covalent **BAM10** complexes to form (which do not simply rely on proximity and non-covalent binding), reducing the ability of ThioLox to competitively displace the **BAM10**.

Investigating Novel Protein Targets in Vivo

Finally, we set out to explore whether **BAM10** can be used as a probe to detect lipoxygenases in another model system. *Caenorhabditis elegans* (*C. elegans*) is one of the most extensively studied systems in biology, known for its ease of culture and manipulation, as well as its suitability for *in vivo* imaging. Despite these advantages, there are currently no reported enzymes with lipoxygenase activity from *C. elegans.* Initially, we performed a BLAST analysis to identify *C. elegans* genes that share sequence identity with 15-LOX-1. This analysis identified four uncharacterized genes with sequence identities ranging from 28 % to 36 %; F07C6.4, F44B9.8, M70.1 and M70.3 (Figure 6e and Figure S15). Encouraged by this, we first assessed whether **BAM10**, supplemented in the food source, could be taken up by the worms. *In vivo* imaging of **BAM10**-treated animals showed increased fluorescence in the pharynx and the intestine, which was significantly higher than the background (Figure 6f and Figure S16b). Crucially, 5 μM **BAM10** did not cause any development delay in the worms, as opposed to paraquat-treated animals used as a negative control (Figure 6g and Figure S16a). Subsequently, we performed competition experiments, using both **BAM3** and **ThioLox**, to explore whether the labelling corresponded to specific binding. For these experiments, we focused on quantifying the fluorescence in the pharynx as it can be easily distinguished and it is the first organ that **BAM10** reaches upon ingestion. Consistent with our cellular experiments, both competitors reduced **BAM10** fluorescence intensity, with ThioLox being, once again, more effective (Figure 6h). Lastly, in order to explore whether the observed binding involves any of the hits from BLAST, we performed reverse genetics experiments where individual genes are down-regulated by RNA interference (RNAi). We reasoned that if **BAM10** labelling is related to any of the genes, then its labelling should decrease if the corresponding protein levels are reduced. Using the Ahringer RNAi library, we obtained three out of the four RNAi constructs (excluding M70.1) and used these in *C. elegans.* Worms grown on RNAi plates were treated with **BAM10** and images were subsequently taken. Imaging analysis revealed that the fluorescence intensity of **BAM10** decreased upon F07C6.4 and M70.3 RNAi (as opposed to F44B9.8 RNAi) (Figure 6h). As both genes are uncharacterized, we used the AlphaFold3 server to predict their potential to bind lipids, using oleic acid as a model substrate, as it is the only available unsaturated lipid in the server. As a control, we initially performed the

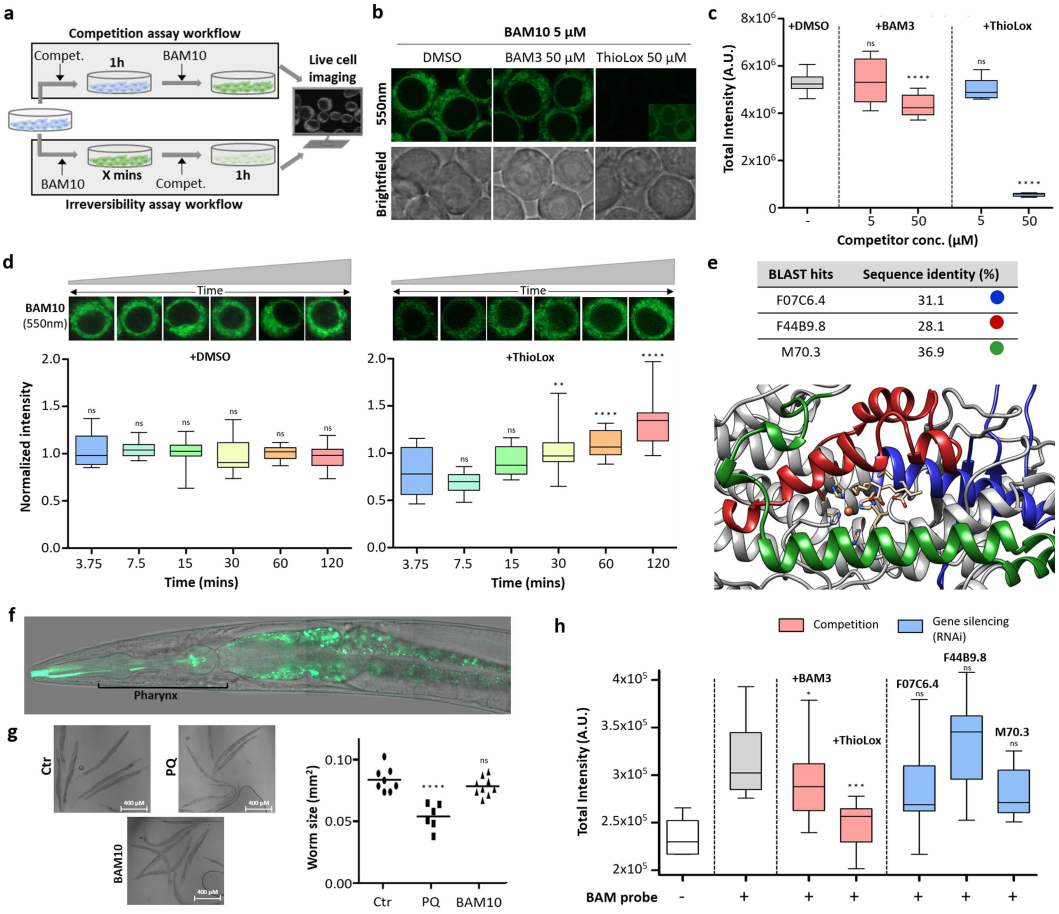

Figure 6. BAM10 in live cell and *in vivo* imaging applications. a) Workflows for competition and irreversibility assays to assess *in cellulo* target engagement of 15-LOX-1 by BAM10, using confocal microscopy. RAW 264.7 cells were seeded on glass-bottom dishes and treated *in situ*. b) Representative images of live cells pre-treated with either DMSO or BAM3 (50 µM) or Thiolox (50 µM) and subsequently labelled with 5 µM BAM10. c) Boxplot showing the quantified intensity per cell area from experiments in b. d) Irreversibility assay where live cells were initially incubated with BAM10 for various durations (3.75 to 120 minutes) and then treated with DMSO or ThioLox (50 µM) for 1 hour before imaging. e) BLAST results showing *C. elegans* genes with high sequence identity to 15-LOX-1. Colored sequence regions correspond to the highlighted colored areas in the 15-LOX-1 structure. f) 16-hour incubation of *C. elegans* with BAM10 leads to significantly higher fluorescence intensity on the pharynx and the intestine. g) Stereoscope images of *C. elegans* on NGM plates treated with DMSO (Ctr), paraquat (PQ) or BAM10. *C. elegans* grown on BAM10 reached similar sizes and showed normal egg development in their gonads, comparable to control samples. Additionally, unlike the negative control (PQ-treated plates), BAM10 does not appear to repel animals from the food source. h) Box-plot of the quantified intensity per area from experiments using 5 µM BAM10 (left) pre-incubated with DMSO or BAM3 (50 µM) or Thiolox (50 µM), (right) on RNAi constructs. Cell culture experiments were performed in triplicates ($n = 3$). Seven or more cell areas were acquired per replicate. For the *C. elegans* experiments, up to 25 animals per condition were used. *$p < 0.05$, **$p < 0.01$, ***$p < 0.001$, and ****$p < 0.0001$.

binding prediction for 15-LOX-1. As expected, 15-LOX-1 is predicted to bind the lipid with high confidence, the binding site of which is located in the same pocket as previously crystallized rabbit LOX (PBD: 1LOX, 2P0M) (Figure S17). Among the *C. elegans* genes used in the AlphaFold3 server, M70.3 has the most appropriate values above the threshold for a reliable model. These results demonstrate for the first time the existence of unknown enzymes with potential lipoxygenase activity in *C. elegans*, underlining the unique applicability of **BAM10** to animal systems.

Conclusion

The discovery and optimization of small molecule modulators have traditionally been hampered by challenges such as lack of specificity, poor pharmacokinetics, and the time-intensive nature of conventional screening processes. In this work, we addressed these limitations by developing a streamlined and efficient methodology designed to enhance the discovery of molecules with improved properties. Our approach leverages MCRs to rapidly, in a single step, generate a diverse library of tool compounds. This innovation enables the simultaneous exploration of a broad chemical space, thereby increasing the likelihood of identifying potent and specific molecules.

Herein, we generated a versatile chemical toolbox by incorporating the BA moiety, a known selective covalent warhead for human 15-LOX-1. This is an essential enzyme that occupies a central role in regulating crucial mechanistic pathways associated with a wide array of pathologies. Fully understanding the role of this enzyme in these complex pathways requires small molecules that can modulate its function. By performing cheminformatic analysis of previous 15-LOX-1 inhibitors and harnessing this selective covalent warhead, we synthesized and characterized a range of BAM compounds. These compounds have incorporated strategic elements, endowing them with different unique features for protein labeling and on-demand inhibition. We fully characterized the covalent nature of our compounds, performing enzyme inhibition and kinetic analysis as well as MS-based binding site mapping. Our findings suggest that the attachment site is located at the entrance of the active site, near the iron, specifically involving amino acids Y395, T396, and L397. Among others, we have developed a very potent in the low nanomolar range inhibitor (**BAM3**), along with easy access to a chemo-sensor (**BAM14**), a light-controlled inhibitor (**BAM12**) and a cross-linker (**BAM13**) switching from bio-silent to bioactive forms upon UV irradiation. Most importantly, we have also developed a cell-permeable, non-toxic, activity-based probe (**BAM10**). We have explored the features of this exceptional probe in live cell and *in vivo* imaging applications, demonstrating its ability to label 15-LOX-1 based on its activity, by evaluating known 15-LOX-1 inhibitors, such as **ThioLox**. Additionally, the probe enabled the *in vivo* identification of novel, previously unknown protein targets with potential lipoxygenase-like activity in *C. elegans*.

The versatility and efficiency of our methodology not only facilitate the development of diverse chemical modulators but also open new avenues for drug discovery and biological research. By providing a robust platform for the rapid synthesis of small molecules, this approach significantly increases the potential for discovering therapeutically relevant compounds with desirable specificity and pharmacokinetic profiles. Importantly, our methodology holds significant promise for applications in various protein targets, beyond 15-LOX-1, laying the groundwork for future advancements in the field of chemical biology.

Supporting Information

The authors have cited additional references within the Supporting Information.[61–69]

Acknowledgements

We acknowledge a) the Empeirikeion Foundation, b) the National Recovery and Resilience Plan Greece 2.0, funded by the European Union—NextGenerationEU (project code: TAEDR-0535850) and c) the Hellenic Foundation for Research and Innovation (H.F.R.I.) under the Greece 2.0 Basic Research Financing Action «Horizontal support of all sciences» Sub-action 2 (project number: 15511) for providing grants to N.E and 2nd Call for H.F.R.I. Research Projects to support Post-Doctoral Researchers" (Project Number: 0911) to C.G.N. Work in N.T.'s laboratory is funded by grants from the European Research Council (ERC-GA695190-MANNA), the Hellenic Foundation for Research and Innovation (HFRI—FM17C3-0869, NeuroMitophagy) and the General Secretariat for Research and Innovation of the Greek Ministry of Development and Investments. D.K. is supported by European Research Area (ERA) Postdoctoral Fellowship under Marie Sklodowska-Curie Actions (UnFearHD—Grant agreement ID: 101130833). We acknowledge Prof. T. Holman (University of California, Santa Cruz) for providing the human 15-LOX-1 plasmid. We would also like sincerely thank Dr. Tamsyn Montagnon for her valuable remarks and Proteomics facility at IMBB for the (MS)-based proteomics.

Conflict of Interest

The authors declare no conflict of interest.

Data Availability Statement

The data that support the findings of this study are available in the supplementary material of this article.

Keywords: small molecule modulators · probes · covalent inhibitors · photopharmacology · human 15-lipoxygenase-1

[1] M. R. Arkin, J. A. Wells, *Nat. Rev. Drug Discovery* **2004**, *3*, 301–317.
[2] S. L. Schreiber, *Nat. Chem. Biol.* **2005**, *1*, 64–66.
[3] Y. Tabana, D. Babu, R. Fahlman, A. G. Siraki, K. Barakat, *BMC Biotechnol.* **2023**, *23*, 44.
[4] K. Wu, E. Karapetyan, J. Schloss, J. Vadgama, Y. Wu, *Drug Discovery Today* **2023**, *28*, 103730.
[5] F. Sutanto, M. Konstantinidou, A. Dömling, *RSC Med. Chem.* **2020**, *11*, 876–884.
[6] E. O. J. Porta, P. G. Steel, *Curr. Res. Pharmacol. Drug Discov.* **2023**, *5*, 100164.
[7] A. J. van der Zouwen, M. D. Witte, *Front. Chem.* **2021**, *9*, 1–17.
[8] D. Wu, A. C. Sedgwick, T. Gunnlaugsson, E. U. Akkaya, J. Yoon, T. D. James, *Chem. Soc. Rev.* **2017**, *46*, 7105–7123.
[9] J. Volarić, W. Szymanski, N. A. Simeth, B. L. Feringa, *Chem. Soc. Rev.* **2021**, *50*, 12377–12449.
[10] H. Guo, Z. Li, *MedChemComm* **2017**, *8*, 1585–1591.
[11] L. Zhong, Y. Li, L. Xiong, W. Wang, M. Wu, T. Yuan, W. Yang, C. Tian, Z. Miao, T. Wang, et al., *Signal Transduct. Target. Ther.* **2021**, *6*, 201.
[12] T. S. Maurer, M. Edwards, D. Hepworth, P. Verhoest, C. M. N. Allerton, *Drug Discovery Today* **2022**, *27*, 538–546.
[13] N. Eleftheriadis, S. A. Thee, M. R. H. Zwinderman, N. G. J. Leus, F. J. Dekker, *Angew. Chem. Int. Ed.* **2016**, *55*, 12300–12305.
[14] B. Samuelsson, S. E. Dahlén, J. A. Lindgren, C. A. Rouzer, C. N. Serhan, *Science* **1987**, *237*, 1171–1176.
[15] E. Sigal, C. W. Laughton, M. A. Mulkins, *Ann. N.Y. Acad. Sci.* **1994**, *714*, 211–24.

[16] J. Z. Haeggström, C. D. Funk, *Chem. Rev.* **2011**, *111*, 5866–5898.
[17] F. Mao, Y. Wu, X. Tang, J. Wang, Z. Pan, P. Zhang, B. Zhang, Y. Yan, X. Zhang, H. Qian, et al., *Biotechnol. Lett.* **2017**, *39*, 929–938.
[18] J. Zhao, V. B. O'Donnell, S. Balzar, C. M. St. Croix, J. B. Trudeau, S. E. Wenzel, *Proc. Natl. Acad. Sci. USA* **2011**, *108*, 14246–14251.
[19] U. Mabalirajan, R. Rehman, T. Ahmad, S. Kumar, G. D. Leishangthem, S. Singh, A. K. Dinda, S. Biswal, A. Agrawal, B. Ghosh, *Sci. Rep.* **2013**, *3*, 1540.
[20] A. R. Lindley, M. Crapster-Pregont, Y. Liu, D. A. Kuperman, *Mediators Inflammation* **2010**, *2010*, 727305.
[21] K. van Leyen, *CNS Neurol. Disord. Drug Targets* **2013**, *12*, 191–199.
[22] P. F. Giannopoulos, Y. B. Joshi, J. Chu, D. Praticò, *Aging Cell* **2013**, *12*, 1082–1090.
[23] Y. B. Joshi, P. F. Giannopoulos, D. Praticò, *Trends Pharmacol. Sci.* **2015**, *36*, 181–186.
[24] D. Praticò, V. Zhukareva, Y. Yao, K. Uryu, C. D. Funk, J. A. Lawson, J. Q. Trojanowski, V. M.-Y. Lee, *Am. J. Pathol.* **2004**, *164*, 1655–1662.
[25] K. van Leyen, H. Y. Kim, S.-R. Lee, G. Jin, K. Arai, E. H. Lo, *Stroke* **2006**, *37*, 3014–3018.
[26] A. Fiedorowicz, H. Car, S. Prokopiuk, E. Sacharzewska, M. Żendzian, K. Kowal, *Prog Heal. Sci* **2013**, *3*, 33–38.
[27] K. van Leyen, K. Arai, G. Jin, V. Kenyon, B. Gerstner, P. A. Rosenberg, T. R. Holman, E. H. Lo, *J. Neurosci. Res.* **2008**, *86*, 904–909.
[28] S. Tobaben, J. Grohm, A. Seiler, M. Conrad, N. Plesnila, C. Culmsee, *Cell Death Differ.* **2011**, *18*, 282–292.
[29] F. Succol, D. Praticò, *J. Neurochem.* **2007**, *103*, 380–387.
[30] J. Chu, J.-G. Li, P. F. Giannopoulos, B. E. Blass, W. Childers, M. Abou-Gharbia, D. Praticò, *Mol. Psychiatry* **2015**, *20*, 1329–1338.
[31] A. J. Klil-Drori, A. Ariel, *Prostaglandins Other Lipid Mediators* **2013**, *106*, 16–22.
[32] M. A. Vaezi, B. Safizadeh, A. R. Eghtedari, S. S. Ghorbanhosseini, M. Rastegar, V. Salimi, M. Tavakoli-Yaraki, *Lipids Health Dis.* **2021**, *20*, 169.
[33] H.-E. Claesson, W. J. Griffiths, Å. Brunnström, F. Schain, E. Andersson, S. Feltenmark, H. A. Johnson, A. Porwit, J. Sjöberg, M. Björkholm, *FEBS J.* **2008**, *275*, 4222–4234.
[34] F. Schain, D. Schain, Y. Mahshid, C. Liu, A. Porwit, D. Xu, H.-E. Claesson, C. Sundström, M. Björkholm, J. Sjöberg, *Clin. Lymphoma Myeloma* **2008**, *8*, 340–347.
[35] Y. Chen, C. Peng, S. A. Abraham, Y. Shan, Z. Guo, N. Desouza, G. Cheloni, D. Li, T. L. Holyoake, S. Li, *J. Clin. Invest.* **2014**, *124*, 3847–3862.
[36] S. V. K. Mahipal, J. Subhashini, M. C. Reddy, M. M. Reddy, K. Anilkumar, K. R. Roy, G. V. Reddy, P. Reddanna, *Biochem. Pharmacol.* **2007**, *74*, 202–214.
[37] D. Li, Y. Li, *Signal Transduct. Target. Ther.* **2020**, *5*, 108.
[38] L. Probst, J. Dächert, B. Schenk, S. Fulda, *Biochem. Pharmacol.* **2017**, *140*, 41–52.
[39] W. S. Yang, K. J. Kim, M. M. Gaschler, M. Patel, M. S. Shchepinov, B. R. Stockwell, *Proc. Nat. Acad. Sci.* **2016**, *113*, E4966–E4975.
[40] H. Feng, B. R. Stockwell, *PLoS Biol.* **2018**, *16*, e2006203.
[41] D. Chen, Z. Xiao, H. Guo, D. Gogishvili, R. Setroikromo, P. E. van der Wouden, F. J. Dekker, *Angew. Chem. Int. Ed.* **2021**, *60*, 21875–21883.
[42] M. J. Schilstra, W. F. Nieuwenhuizen, G. A. Veldink, J. F. G. Vliegenthart, *Biochemistry* **1996**, *35*, 3396–3401.
[43] A. Boltjes, A. Dömling, *Eur. J. Org. Chem.* **2019**, *2019*, 7007–7049.
[44] C. G. Neochoritis, T. Zhao, A. Dömling, *Chem. Rev.* **2019**, *119*, 1970–2042.
[45] L. V. Myznikov, A. Hrabalek, G. I. Koldobskii, *Chem. Heterocycl. Compd.* **2007**, *43*, 1–9.
[46] W. Tong, Q.-Y. Li, Y.-L. Xu, H.-S. Wang, Y.-Y. Chen, Y.-M. Pan, *Adv. Synth. Catal.* **2017**, *359*, 4025–4035.
[47] N. Eleftheriadis, C. G. Neochoritis, N. G. J. Leus, P. E. van der Wouden, A. Dömling, F. J. Dekker, *J. Med. Chem.* **2015**, *58*, 7850–7862.
[48] N. Eleftheriadis, H. Poelman, N. G. J. Leus, B. Honrath, C. G. Neochoritis, A. Dolga, A. Dömling, F. J. Dekker, *Eur. J. Med. Chem.* **2016**, *122*, 786–801.
[49] N. Eleftheriadis, S. Thee, J. te Biesebeek, P. van der Wouden, B.-J. J. Baas, F. J. Dekker, *Eur. J. Med. Chem.* **2015**, *94*, 265–275.
[50] R. van der Vlag, H. Guo, U. Hapko, N. Eleftheriadis, L. Monjas, F. J. Dekker, A. K. H. Hirsch, *Eur. J. Med. Chem.* **2019**, *174*, 45–55.
[51] A. Shevchenko, H. Tomas, J. Havli, J. V. Olsen, M. Mann, *Nat. Protoc.* **2006**, *1*, 2856–2860.
[52] A. Golovanov, A. Zhuravlev, A. Cruz, V. Aksenov, R. Shafiullina, K. R. Kakularam, J. M. Lluch, H. Kuhn, À. González-Lafont, I. Ivanov, *J. Med. Chem.* **2022**, *65*, 1979–1995.
[53] M. M. Gleason, C. J. Rojas, K. S. Learn, M. H. Perrone, G. E. Bilder, *Am. J. Physiol. Physiol.* **1995**, *268*, C1301–C1307.
[54] K. Traven, N. Eleftheriadis, S. Seršen, J. Kljun, J. Bezenšek, B. Stanovnik, I. Turel, F. J. Dekker, *Polyhedron* **2015**, *101*, 306–313.
[55] R. E. Bird, S. A. Lemmel, X. Yu, Q. A. Zhou, *Bioconjugate Chem.* **2021**, *32*, 2457–2479.
[56] H. Fang, B. Peng, S. Y. Ong, Q. Wu, L. Li, S. Q. Yao, *Chem. Sci.* **2021**, *12*, 8288–8310.
[57] S. Heinzlmeir, S. Müller, *Drug Discovery Today* **2022**, *27*, 519–528.
[58] D. Cao, Z. Liu, P. Verwilst, S. Koo, P. Jangjili, J. S. Kim, W. Lin, *Chem. Rev.* **2019**, *119*, 10403–10519.
[59] W. A. Velema, W. Szymanski, B. L. Feringa, *J. Am. Chem. Soc.* **2014**, *136*, 2178–2191.
[60] H. Guo, I. C. Verhoek, G. G. H. Prins, R. van der Vlag, P. E. van der Wouden, R. van Merkerk, W. J. Quax, P. Olinga, A. K. H. Hirsch, F. J. Dekker, *J. Med. Chem.* **2019**, *62*, 4624–4637.

Manuscript received: September 23, 2024
Accepted manuscript online: November 11, 2024
Version of record online: November 22, 2024